Manuscript accepted by *Hydrologic Processes* February 5, 1999

CORRELATION LENGTHS OF MELTWATER FLOW THROUGH RIPE SNOWPACKS, COLORADO FRONT RANGE, USA

Mark W. Williams
Institute of Arctic and Alpine Research and
Department of Geography, CB 450,
University of Colorado, Boulder, CO

Richard Sommerfeld
Rocky Mountain Forest and Range Experimental Station
US Forest Service, Department of Agriculture
Fort Collins, CO

Sam Massman
Institute of Arctic and Alpine Research and
Department of Geography, CB 450,
University of Colorado, Boulder, CO

Mark Rikkers
Institute of Arctic and Alpine Research and
Department of Geography, CB 450,
University of Colorado, Boulder, CO

Corresponding Address†

Mark W. Williams
INSTAAR and Dept. of Geography
Campus Box 450
Boulder, CO 80309-0450
Telephone: 303/492-8830

ABSTRACT

The flowpaths of meltwater through snow is known to be an inhomogeneous process. The spatial distribution of meltwater flowing from the bottom of melting snowpacks is the result of horizontal and vertical flow paths within the snowpack. The ability to characterize the spatial distribution of these meltwater flowpaths would be useful in developing models of snow melt runoff which could better characterize snow melt hydrographs. We analyzed near infrared aerial photos of melting snow using a moving window analysis which can characterize correlation lengths in the reflectance of the snow surface. Near infrared is sensitive to snow grain size, which in turn may indicate higher amounts of melt water; the grains grow faster if the liquid water content is higher. Correlation lengths were 5-7 m and the probability of finding such correlation lengths increased from 0.22 in May, 1997 when the melt had just started to 0.68 by late June when melt was well established. Liquid water content at the snow surface was sampled with a dielectric sensor at 0.5 m intervals on 100-m^2 and 75-m^2 grids. Semi-variograms showed a sill at 5 to 6 meters. The liquid water measurements at the snow surface suggest that the correlation lengths derived from the infrared aerial photos represent surface expressions of higher flow density through the melting snowpack. A circular array of 16 snow melt lysimeters each with areas of 0.2 m^2 was operated for two years at Niwot Ridge in the Colorado Front Range. Variograms indicated that flows were correlated over a distance of 5 to 7 m. These three independent methods all suggest a spatial oganization of 5-7 m for flowpaths draining ripe snowpacks in the Rocky Mountains.

INTRODUCTION

The movement of water through the snowpack is one of the least understood aspects of snow hydrology [Colbeck, 1975]. Considerable effort has been devoted to improving our understanding of the fundamental physics underlying infiltration processes in snowpacks [e.g. Colbeck 1971, 1972; Ambach et al., 1981; Colbeck and Anderson, 1982; Jordan, 1983a,b]. The physical processes of snow melting and water infiltration in snow involve a complex mixture of snowpack thinning during the melting cycle, water flow through a variably saturated porous medium, refreezing of meltwater by subfreezing internal temperatures and the surface freezing cycle, and changes in the hydraulic and thermal properties of snow due to meltwater refreezing [Kattelmann, 1995]. In addition, snowpacks are highly heterogeneous due to both macroscopic layering and smaller-scale variations in bulk density and grain structure. As yet, little progress has been made in carrying out theoretical or experimental studies which quantify the relevant physical processes under natural field conditions.

Movement of liquid water through snowpacks is generally recognized to occur in distinct flow paths rather than as uniform flow through a homogeneous porous medium. Seligman [1936] found that snowpack permeability was enhanced when flow channels were present in the snowpack. Oda and Kudo [1941] described flow fingers and flow along layer interfaces. Dye was used to trace flow paths during the Cooperative Snow Investigations [Gerdel, 1948 and 1954; US Army, 1956]. Ice columns, described previously by Ahlmann and Tveten [1923], Ahlmann [1935], Seligman [1936], and Gerdel [1948], were recognized to be the residual flow network in cold snow by Sharp [1951]. Grain growth in paths of preferential flow was related to higher permeability and more efficient flow [Wakahama, 1968*a*]. Saturated conditions and non-Darcy flow were also observed in these flow paths [Wakahama, 1968*b*]. Heat transfer and alteration of snowpack structure by freezing during infiltration have been investigated by Colbeck [1976], Illangasakare et al. [1990], and Pfeffer et al. [1990, 1991]. Zones of preferential flow and ice columns have been observed in many other studies [e.g. Wankiewicz, 1976; Jordan, 1978; Denoth et al., 1979; Higuchi and Tanaka, 1982; Marsh, 1982 and 1988; Kattelmann, 1985 and 1986].

Marsh and Woo [1985] attempted to assess the variability of meltwater flow in Arctic snowpacks using lysimeters with collection areas of 1 m^2, 0.25 m^2, and a third

0.25-m^2 lysimeter which was subdivided into 16 cells each 0.015 m^2 in area. The flow into individual compartments ranged from 0 to 240% of the mean flow with no spatial pattern. However, daily flows among the three lysimeters were generally within 10% of each other. Kattelmann [1989] studied the spatial variability of snow pack outflow at a montane site in the Sierra Nevada, using 4 snow lysimeters each 6-m^2 in area and with two of the lysimeters subdivided into 2-m^2 areas. He reports that meltwater output from a snowpack appears to be highly variable, and that this variability is on a much larger scale than was previously recognized. Because of this high spatial variability in meltwater output from snowpacks in the Sierra Nevada, Kattelmann [1989] recommends the use of snow melt lysimeters that are greater in area than 6 m^2. Furthermore, Bloschl [1999, in press] states that snow lysimeter data at the plot scale is unlikely to capture the large scale variability of snow melt that is due to the larger scale of topography and climatic conditions, and will therefore underestimate the correlation lengths of the underlying true pattern of snow melt in the region.

Our objective here is to evaluate the possibility that meltwater flow through snow may be spatially organized at scales larger than those measured by Marsh and Woo [1985] and Kattelmann [1989]. Direct measurements of the spatial distribution of meltwater movement through snow are difficult. Here we investigate the possibility that there may be some spatial organization in meltwater flow through snow by measuring three inferential and independent parameters: [1] Depressions in the snow surface that may indicate preferential flowpaths; [2] Liquid water content of the snow surface; and [3] Meltwater discharge from the base of the snowpack before contact with the ground in snowpack lysimeters (*e.g.* the technique of Marsh and Woo [1985] and Kattelmann [1989]).

The grain size of wet snow increases rapidly compared to drier snow [Wakahama, 1968a; Colbeck, 1973, 1975, 1976; Marsh, 1987]. The rapid settlement of the snowpack caused by the formation of the coarse grain clusters may produce pits or valley-shaped depressions in the snow surface above them, a phenomenon reported by Seligman [1936] and Gerdel [1948]. Preferential settling of the overlying snow surface may then occur as liquid water penetrates the lower snow layers, providing a visual impression of the drainage loci within the snowpack [Wankiewicz, 1979]. Accumulating lateral flow may then occur between the depressions, with greater flow amounts at the depressions.

Kattelmann [1989] reports that in a mult-lysimeter study conducted in the Sierra Nevada a similar depression formed over a collector that consequently received a greater volume of melt water than the other lysimeters.

These valleys or depressions on the snow surface may provide an index for the spatial organization of meltwater flow through snow. Little quantitative information exists on the spatial distribution of these valleys or depressions. Wankiewicz [1979] suggests a repeating linear distance of 3 m between vertical flowpaths and overlying valleys on a sloped and draining snowpack. Wankiewicz [1979] also suggests that there may be a consistent repeating distance between these vertical flowpaths and their overlying surface depressions that is analogous to wavelength, such that vertical flowpaths and overlying surface depressions in a ripe and draining snowpack are separated by a characteristic wavelength (λ) that is the average linear distance between vertical flowpaths (Figure 1).

Remote sensing techniques may provide a method of distinguishing these depressions from raised areas on the snow surface. The reflectivity of snow decreases with increasing grain size in the near infrared (0.8 to 2.4 μm) because ice is moderately absorptive in those wavelengths [Nolin and Dozier, 1993]. Dozier [1989] documented the change in grain size for the seasonal snowpack in the Kern River drainage of the Sierra Nevada over the snow accumulation and melt season using the changes in reflectance values of snow-covered area obtained from Landsat imagery. The combination of depressions with larger snow grains and peaks with smaller snow grains suggests that there may be large differences in albedo between these two areas of the snow surface. Sommerfeld et al. [1994] hypothesized that the larger grain sizes in surface depressions caused by the concentration of liquid water should cause a bimodal brightness distribution in infrared aerial photos of melting snow. They further hypothesized that the separation of the brightness values would be maximized by spatially filtering the images with a filter sized according to the spacing of the surface depressions. They supported this hypothesis with reflectance values of snow-covered areas in both visible and infra-red aerial photographs. It is unclear whether these observations were caused by actual differences in surface wetness, however the measured reflectance values demonstrated spatial organization with a correlation length of about 6 m. Additionally, the quantity of their data was small and the question of the consistency of the correlation distance over wider areas remains open.

Measurements of other snowpack parameters that would supply ground-truth verification were missing from the research of Sommerfeld et al. [1994]. We used a dielectric sensor to determine if there was a spatial pattern in the liquid water content of the snow surface. A number of investigators have used dielectric methods to measure the liquid water content of the snow surface, but to our knowledge none have used a systematic sampling scheme to understand the spatial distribution [*e.g.* Denoth et al., 1984; Boyne and Fisk, 1987; Kattelmann, 1990]. We use a geostatistical approach to evaluate whether or not there is any spatial organization of the liquid water measurements. Semivariograms provide a quantitative method of estimating the spatial distance at which liquid water measurements may be related.

Measurements of the timing and magnitude of meltwater outflow at the base of the snowpack also provide a surrogate for understanding the spatial distribution of meltwater flow through snow [*e.g.* Marsh and Woo, 1985; Kattelmann, 1989]. However, construction of snow lysimeters larger than the 6 m^2 used by Kattelmann [1989] is problematic because the presence of the lysimeter itself can affect physical processes that influence snowpack properties and structure, such as heat and vapor exchanges between the snowpack and underlying surface. Consequently, we measure the meltwater outflow from the base of the snowpack using lysimeters deployed in a geometrical array. This experimental design allows us to sample a larger spatial area while minimizing artifacts caused by the experimental apparatus, compared to more traditional designs such as subdividing a large snow lysimeter into smaller compartments. Again, we can use a geostatistical approach to analyze the data for any spatial dependencies.

The correlation length of 6 m for meltwater flowing through ripe snowpacks reported by Sommerfeld et al. [1994] was surprisingly large compared to the much smaller spatial separation in flow-fingers and macropores reported by Kattelmann [1985], Marsh and Woo [1985], and McGurk and Marsh [1995]. We test these null hypotheses: [1] The characteristic distance separating bimodal reflectance peaks from aerial photographs of a draining snowpack in Colorado will not be the same as that reported by Sommerfeld et al. [1994] for a Wyoming snowpack (*e.g* results reported by Sommerfeld et al. [1994] were site specific). [2] The frequency of bimodal distribution of brightness values from aerial photographs of snow covered area will not increase from early in the melt season to later in the melt season as meltwater flowpaths became more established. [3] Direct measurements of the liquid water content of the snow surface will a) have no

spatial structure, and b) if there is spatial structure it will not have the same characteristic distance as bimodal distributions of brightness values. [4] The correlation length of meltwater discharge measured in snow lysimeters at the base of the snowpack will not be the same as the bimodal brightness distribution of aerial photographs. Here we are using measured values of the liquid water content of the snow surface and the outflow of snow lysimeters as ground truth for the analysis of the aerial photographs.

SITE DESCRIPTION

All experiments were conducted on Niwot Ridge, located in the Colorado Front Range of the Rocky Mountains about 5 km east of the Continental Divide (40° 03' N, 105° 35' W) (Figure 2). This site is an UNESCO Biosphere Reserve and a Long-Term Ecological Research (LTER) network site. Climate is characterized by long, cool winters and a short growing season (1-3 months). Mean annual temperature is -3.8°C and annual precipitation is 1,000 mm [Williams et al., 1996a]. About 80% of annual precipitation falls as snow [Caine, 1996].

Niwot Ridge is an alpine interflueve and was not glaciated during the Pleistocene; it extends from the continental divide at an elevation of 3,700 m east about 6 km to an elevation of 3,400 m (Figure 2). Aerial photographs were taken of the alpine area shown in Figure 2, which is about 2 km in length west to east and 0.5 km in length south to north. Slope angles range from about 0 to 15° with a median of about 4°; azimuth ranges from 0 to 365° with slopes predominantly flat to east-facing. A meteorological station, subnivean laboratory, snow lysimeter array, and index snowpit site are located on the Saddle area (Figure 2). This research area is flat and continuous with terrain that gradually increases in slope to about 15° at the top of the West Knoll about 400 m to the west of the Saddle research site. The snow at the research area is not isolated from the surrounding snowpack, following the protocol of Schneebeli [1998].

DATA ANALYSIS

One needs an objective criterion for rejecting or not rejecting the null hypothesis for a particular statistical test. Statistical tests calculate the probability (p) of a particular event occurring. The probability used as the criterion for rejection of the null hypothesis is termed the significance level (α) [Zar, 1984]. Here use $\alpha = 0.05$ as the significance

level, or the probability of an event occurring must be less than 1 in 20. Additionally, a requirement for parametric tests such as a t-test of means or an F-test of variances is that the data be normally distributed (bell-shaped frequency curve).

Geostatistics provides a means of understanding the geographic distribution of a variable such as snow depth or meltwater flow through snow. The semivariance is a measure of the degree of spatial dependence among samples as a function of distance. Conceptually, samples are uniformly spaced along straight lines at some uniform distance Δh. The semivariance (γ_h) can then be estimated for distances that are multiples of Δh (or the linear lag distance), as the sum of the squared differences between pairs of points separated by the distance Δh [Davis, 1986]. If we calculate the semivariance for different values of h, we can plot the results in the form of a semivariogram. Points close to each other tend to be very similar and have a small semivariance. At some distance the points being compared are so far apart that they are not related to each other and the semivariance becomes equal to the variance around the average value. The semivariance no longer increases and the semi-variogram develops a flat region called a sill. The linear distance (or range) at which the semivariance approaches the variance (the sill) defines a spatial range within which all locations are related to one another. In practice, semivariances can be calculated for any distance, whether samples are a multiple of Δh or not. While geostatistics provide a quantitative method of evaluating the spatial dependencies of a variable, they cannot be used to test whether variables are significantly different [Davis, 1986].

Following Bloschl and Sivapalan [1995] and Bloschl [1999, in press], we suggest that the measurement scale for our geostatistical analyses consists of "spacing", "extent", and "support". "Spacing" refers to the distance between samples, "extent" refers to the distance over which the samples are made, and "support" refers to the area of the individual sample measurements.

Spectral analysis is the partioning of the variation in a regular repeating series into components according to the duration or length of the intervals within which the variation occurs [Davis, 1986]. Spectral analysis is known by various names, including harmonic analysis, Fourier analysis, and frequency analysis. The distance from a point on one wave form to the equivalent point on the next wave form is called the wavelength, λ. Here the length of a wavelength identified by Fourier analysis is the same as the distance

or wavelength λ of successive vertical flowpaths in a draining snowpack as suggested by Wankiewicz [1979] (Figure 1). Fourier analysis of spatial data can also be used to filter the data, that is to smooth a data set such that "short-term" or "high frequency" noise is removed from the data set to reveal an underlying "long-term" signal.

Remotely-sensed data provides a non-destructive method of sampling some snow properties over large areas. Here we adapt the approach of Dozier [1989] to distinguish the spatial distribution of valleys or depressions on the snow surface composed of large grains from raised areas on the snow surface that are composed of smaller grains. We apply a Fourier analysis to the brightness signal recorded by aerial photographs, using a modified version that reduces computational time, called a fast Fourier transform or FFT. Our objectives with the Fourier analysis of aerial photographs were to a) look for repeating patterns in light intensity (brightness value), and b) as a filter to remove higher-frequency patterns. Remote sensing images of snow-covered area using space-borne sensors are not appropriate for this analysis because the pixel size of Landsat (30 m) and AVHRR (1,000 m) are larger than the spacing of flowpaths in a ripe and draining snowpack.

METHODS

Snowpack conditions are monitored about weekly at the Saddle site on Niwot Ridge (Figure 2) following the protocol of Williams et al. [1996b]. Snow water equivalence (SWE) measurements are made using a 1-L stainless steel cutter in vertical increments of 10 cm [Williams and Melack, 1991]. Temperature of the snowpack is measured every 10 cm with 20-cm long dial stem thermometers, calibrated to ± 0.2°C using a one-point calibration at 0°C. Grain type, size, and snowpack stratigraphy are also recorded. Depth-weighted values are then calculated for snowpack density, temperature, and water equivalent. Raw and calculated values, along with additional information on methods, are available at the Niwot Ridge LTER site (http://culter.Colorado.EDU:1030/Subnivean/) [Williams et al. (in review)].

Aerial Photographs

Aerial photographs of snow-covered area were acquired using a 70-mm Kodak Infrared Aerographic type 2424 film. The camera was a motor drive Hasselblad, with a 250-mm lense. Visible light sensitivity was attenuated with a yellow filter (Wratten No.

12) resulting in a spectral response of approximately 900 to 1200 nm. Aerial photographs were taken at an altitude of 5,000 m m.a.s.l. (or about 1,500 m above the study area) on three dates: 14 June 1995, 13 May 1997, and 24 June 1997.

Black and white negatives from the three flights were digitized using a Sony 3 CCD color video camera with a resolution of 640 X 780 pixels per frame. The resulting scale factor, 570 mm pixel, was determined by ground and map measurements of identifiable features. Camera images were acquired in ImagePro Plus (Media Cybernetics, 1995) as grey scale images. The software includes a fast Fourier transform capability. The resulting two dimensional spectrum was edited in the low pass mode to selectively remove higher spatial frequencies.

A checkerboard analogy provides a good example of how we evaluated the brightness levels after the Fourier analysis. The entire checkerboard is a subset of the frame or "window". Raised areas of the snowpack should have smaller grains and a higher albedo and represent the white blocks on a checkerboard (see Figure 1). Depressions should have larger grains and a lower albedo and represent the black boxes on a checkerboard. One wavelength (λ) of light intensity from a checkerboard would then be the length of a white box plus the length of a black box; you then reach the beginning of the next white box or the start of the next wavelength. The brightness values of the white box at any point on the white box would be correlated with itself but not correlated with the light intensity of the black box. The correlation length for brightness values of the white box would then be the length of the white box, or 1/2 λ; with the same relationship holding for the black box.

We then construct a frequency diagram of brightness values for that window. We will get a bimodal distribution of brightness values if the spatial filter is about the length of one black box plus one white box of the checkerboard. If the spatial filter is larger or smaller that the length of the two boxes, we get a bell-shaped frequency distribution. If the snow surface is not composed of alternating dark and light patches, again we will not obtain a bimodal distribution of brightness values. Figure 3 shows an example from Sommerfeld et al. [1994] of how the frequency distribution of brightness values changes by changing the size of the spatial filter used in the Fourier analysis. At a wavelength of 1.5 m there is a single peak in the frequency of brightness values. As the size of the spatial filter increases the frequency distribution of brightness values changes, with a

strongly bimodal distribution at a wavelength of 12 m or correlation length of 6 m.

No formal method was used to randomize this survey. However, the aircraft pilot made no attempt to acquire images of specific areas and the only criteria used to select frames for analysis was (1) the frame was largely snow covered and (2) it did not significantly overlap other analyzed frames. It is thus unlikely that there was any bias in the image selection.

Liquid Water Content of Snow Surface

The liquid water content of the snow surface was measured with a portable dielectric sensor, a Finnish Snow Fork [Shivola and Tiuri, 1986]. The snow fork measures the liquid water content at the snow surface to a depth of 60 mm and over an area about 2 cm in diameter. The snow fork was used because the instrument is fully automated with a fast response time, which is important because the liquid water content of the snow surface changes in response to the local energy balance. Accuracy of the liquid water measurements in snow by the the snow fork was assessed by comparison to the more standard Denoth Wetness Sensor [Denoth et al., 1984]. Comparisons between the snow fork and the Denoth wetness meter were made early in the melt season over a variety of snow conditions to insure that the snow fork produced reliable estimates of the liquid water content of the snow surface. We then made gridded measurements of the liquid water content of the surface of a ripe and draining snowpack for geostatistical analysis in late July on a nearly flat area (slope less than 3°) of Niwot Ridge within 200 m of the lysimeter array.

The spatial distribution of the liquid water measurements was evaluated using a variogram as suggested by Bloschl [1999, in press]:

$$\gamma(h) = \frac{1}{2n} \sum_{i=1}^{n} [Z(x_i) - Z(x_i + h)]^2$$

where h is the lag distance between wetness measurements, n is the total number of points, $Z(x_i)$ are the measured wetness values at each point, $Z(x_i + h)$ are the measured wetness values at each point h distance from $Z(x_i)$, and $\gamma(h)$ is the semivariance. The sill of the semivariogram defines the spatial distance which separates measurements which are correlated (less than the sill) from measurements that are not correlated or are independent (equal to or greater than the sill). Using the terminology of Bloschl [1999, in press], the "spacing" was 0.5 m, the "extent" was 10 m and 7.5 m, and the "support" was

4 cm^2 (the area sampled by the snow fork).

Lysimeter Array

During the summer of 1994, a circular array of sixteen snow lysimeters, each 0.2 m^2 in area with 25-cm sidewalls, was installed with a 5-m radius and approximately 2-m spacing along the arc of the circle, as reported in Rikkers et al. [1996]. Previous arrays of lysimeters have generally used a gridded distribution [*e.g.* Marsh and Woo, 1985; Kattelmann, 1989; Sommerfeld et al., 1994]. We used a circular array because there are more combinations of linear lag pairs than with a square array made from the same number of lysimeters. Consequently, the circular array provides the opportunity for more robust geostatistical tests compared to a square array with the same number of lysimeters. The use of a circular array does not mean that we believe meltwater flows through snow in a circular pattern.

The lysimeters were individually plumbed and output routed by gravity into dedicated tipping buckets (Davis Rain Collector II) in a subnivean laboratory. All buckets were mounted, leveled, and drain funnels directed all meltwater through the floor to a gravel bed below. Individual tipping buckets were wired to a Campbell Scientific CR10 data logger and the data storage card was replaced and downloaded weekly. Meltwater flux was recorded as the total number of tips at ten-minute intervals. Tipping buckets were calibrated to volume by slowly pouring a known amount of water into the buckets and recording the number of subsequent tips; one tip was 4.6 ml (precision of about 10%).

The semivariance is not only equal to the average of the squared differences between pairs of points spaced a distance Δh apart, it is also equal to the variance of these distances:

$$\gamma^*(h) = \left[\sum_{i=1}^{N} \frac{(Z(x_i) - \bar{Z})^2}{n}\right] - \left[\frac{1}{2n_h} \sum_{i=1}^{n_h} [Z(x_i + h) - Z(x_i)]^2\right]$$

where h is the lag distance between pairs of lysimeters, n is the total number of points, n_h is the number of pairs, $Z(x_i)$ are the measured flows and $\bar{Z}$ is the mean of the measurements.

Sommerfeld et al. [1994] used this version of the semivariogram to evaluate the spatial correlation of lysimeter outflow from 12 lysimeters underneath a Wyoming

snowpack. Here we analyze our lysimeter results using the same geostatistical test as Sommerfeld et al. [1994] so that we can compare our results to those of Sommerfeld et al. [1994]. The two different semivariograms are equivalent. Here, the point at which γ^*_h crosses 0 and becomes negative is equivalent to the sill. The spatial variability of meltwater flux was calculated for linear lag distances of 0, 1.9, 3.8, 5.5, 7.1, 8.3, 9.2, 9.8, and 10.0 m. Again using the terminology of Bloschl [1999, in press], the "spacing" was about 2 m, the "extent" was 10 m, and the "support" was 0.2 m^2. Computations were made using a computer script (awk) which ran the spatial variogram on each possible combination of pairs at each lag distance at ten minute intervals.

RESULTS

The 1997 snow year was about average, with a maximum snow depth of 2.57 m occurring on 7 May at the index site on the Niwot Ridge saddle. The snowpack became isothermal at 0°C on 10 May, with complete meltout over the lysimeter array in the second week of July. Maximum snow water equivalence (SWE) was 1,016 mm. The 1995 snow year was characterized by heavy spring snowfall and a later melt date, with snow melt starting about 1 June [Cline, 1997]. The 1996 snow year started late, with several small melt events in the autumn months.

Aerial Photographs

Figure 4 illustrates the process of finding the spatial distribution of brightness values in this snow covered image from 14 June 1995. North is to the top of the scene and the photo was taken about 11 AM. The upper left and lower right areas are unaltered sections of the original frame. Black areas are snow-free areas and the gray area is the snow surface. Note that the snow-covered area shows a consistent gray color with no dark or light patches. The upper middle portion of the frame has been transformed after Fourier analysis with a 12-m spatial filter. Note that this portion of the frame shows contrasting patterns of dark and light patches on the snow surface. The Fourier transform with a 12-m spatial filter has resulted in highlighting light and dark areas of the snow surface that occur in "patches" that are larger in spatial extent than the pixel size of the frame.

We’ve highlighted one "window" located just to the upper right of the center of the frame. The window is approximately 150 pixels by 150 pixels, for a total of about 22,500

brightness measurements representing an area on the ground of 7,310 m^2. The inset on the lower left of the frame is a frequency diagram of brightness values for this window; the x-axis of the inset is brightness value and the y-axis is the number of pixels with that brightness value. There is a tri-modal distribution of brightness values shown in the inset histogram.

For this and all frames, we collected similar measurements of the frequency distribution of brightness values by moving the window to different areas of the frame. We then repeated the Fourier transform on the original image at a different spatial filter and again repeated the same analysis for each window at the new spatial frequency. This approach is a labor intensive, trial and error method, that uses the subjective judgement of a trained observer to determine the spatial filter that provides a bimodal distribution of reflectance values (see Figure 3 for an example). We analyzed a total of 30 frames, 10 frames from each aerial survey of snow-covered area, with nine windows per frame and at least three spatial filters per frame, generating more than 1000 frequency histograms of pixel brightness from more than 22.5 x 10^6 brightness values. Here we provide summary information from the three aerial overflights that were conducted just after the initiation of melt at the bottom of the snowpack (13 May 1997), near the height of the melt season (14 June 1995), and near the end of the melt season (24 June 1997). Bimodal distributions of brightness values were found from all three flights. The probability of finding bimodal brightness distributions increased from 0.22 just after the initiation of snow melt to 0.68 near the end of the melt season (Figure 5). The association between the stage of snow melt and the probability of finding a bimodal distribution in the frequency of brightness values was good.

For all three flights the best separation of the modes in the brightness distribution was associated with a correlation lengt of 5 to 7 meters (Figure 6). However, in most frames there was a multi-modal distribution of brightness values. To illustrate, in both Figure 3 and Figure 6 there are multi-modal peaks in the frequency of brightness values. In most cases the lower-magnitude peaks in brightness values were nested within higher-magnitude brightness values with the characteristic distance of 5-7 m. These results suggest that the correlation length of 5-7 meters in the bimodal distribution of brightness values may be composed of higher-frequency patterns in meltwater flow (*e.g.* meltwater flowpaths are "bunched"). That is, there may be a hierarchial structure to meltwater flow through snow such that the correlation length of 5-7 m may be composed of flowpaths

that are organized into groups with spatial dimensions less than 5-7 m.

Liquid Water Content of Snow Surface

We made measurements of the liquid water content of the snow surface to test if there was any spatial organization. Liquid water measurements by the snow fork were comparable to those made by a Denoth meter. Measurements of liquid water content by both instruments were normally distributed at $\alpha = 0.05$ ($p > 0.05$, $n = 48$). A t-test showed that the average liquid water content of 3.7% measured by the Denoth meter was not significantly different than the 4.2% measured by the Snow Fork at $\alpha = 0.05$ ($p = 0.19$, $n = 48$). Additionally, an F-test showed that there was no significant differences in the variances measured by the two instruments at $\alpha = 0.05$ ($p = 0.19$; $n = 48$), although the variances were greater for the snow fork compared to the Denoth meter. These results are similar to comparisons by Denoth et al. [1984], who reported that liquid water measurements by the two instrument types in the Stubai Alps of Austria showed almost identical means, and with the snow fork having a slightly higher standard deviation. Furthermore, the absolute values of liquid water content measured by the snow fork were less important for our statistical analysis than the relative values

After validating the accurracy of the snow fork, we made near-surface measurements of snow wetness on a 10 x 10 m grid ($n = 441$) (Figure 7) and a 10 x 7.5 m grid ($n = 336$). For both grids, measurements were at 0.5-m increments in late July and with the sun directly overhead. Both data sets were normally distributed at $\alpha = 0.05$, with $p = 0.08$ for the 100-m^2 grid and $p = 0.10$ for the 75-m^2 grid. The average liquid water content was similar for both experiments, 9.1% for the larger grid and 8.8% for the smaller grid.

Somewhat surprisingly, the semivariogram analysis indicates that there was spatial organization in the liquid water content of the snow surface (Figure 8). The sample variances differed between the two sites, with the sample variance of the 10 x 10 m grid almost three times that of the 10 x 7.5 m grid. However, even with these large differences in sample variance, both variograms had small values for γ_h for measurements that were close together, indicating that these values for liquid water content were related. The value of γ_h then increased with increasing distance apart of the measurements for both grids. The sill occurred at 5.9 m for the 10 x 10 m grid and 5.2 m for the 10 x 7.5 m grid.

These geostatistical analyses indicate that the liquid water content of the snow surface was correlated at distances from about 0 to 6 m. Moreover, the fact that the range was similar for the two variograms even though there was a large difference in the sample variance provides additional confidence that the correlation lengths were not an artifact of the sampling parameters. In both cases, there was a small change in slope at about 2.5 m, suggesting that the sill at 5 m may in fact be composed of correlation lengths with a higher spatial frequency. The geostatistical analysis suggests that the liquid water content of the snow surface at this time had a spatial organization of about 5-6 m, similar to the correlation lengths derived from aerial photographs of the snow surface during snow melt.

Lysimeter Array

Meltwater discharge was recorded for all 16 lysimeters in 1995, 1996, and 1997. However, meltwater discharge was inconsistent at times in 1996 because of icing problems and these data are not reported. Illustrating with results from 1997 (some of the 1995 data was reported in Rikkers et al. [1996]), meltwater was collected in all lysimeters from 11 May to 5 July. Total measured flow in each of the 16 lysimeters ranged from a low of 420 mm to a high of 16,000 mm (Figure 9), compared to 1,016 mm in the index snowpit.

Figure 10 is a plot of $\gamma^*_{(h)}$ versus lag distance at ten-minute time steps for the entire 1997 (n = 132,156) and 1995 (n = 131,200) melt seasons. For 1997, the $\gamma^*_{(h)}$ values become negative (or reach the sill) at a distance of 5 m. The $\gamma^*_{(h)}$ values then become positive at about 9 m. For the 1995 season, the $\gamma^*_{(h)}$ values become negative at about 6.5 m. Similar to 1997, the $\gamma^*_{(h)}$ values in 1995 approach zero at a lag distance of about 9 meters but do not become positive. The semivariograms from both 1997 and 1995 suggest that meltwater discharge from the base of draining snowpacks is correlated for a distance of 5-7 m.

DISCUSSION

The correlation lengths of 5-7 m that we report from aerial photographs of Niwot Ridge in Colorado are the same as the 5-7 m correlation lengths reported by Sommerfeld et al. [1994] for a Wyoming snowpack. Our results from a more robust data set show the

same correlation lengths in the distribution of reflectance values from snow-covered area that Sommerfeld et al. [1994] reported from a more limited set of reflectance measurements based on exploratory research. Somewhat surprisingly, our results suggest that the findings reported by Sommerfeld et al. [1994] were not site specific. It is unclear how large an area these results apply to. The correlation length of 5-7 m for a bimodal distribution of reflectance values for snow-covered area may apply to reasonably flat terrain in continental, mid-latitude regions.

Furthermore, the spatial patterns that we observed with the Fourier analysis of the aerial photographs are similar to visual descriptions of depressions by other scientists. Gerdel [1954] considered that the dendritic pattern of depressions commonly observed on the snow surface of melting snowpacks indicated the presence of internal flow channels. Higuchi and Tanaka [1982] carried out field observations in the Tateyama Mountains of Japan on the morphological regularity of dendritic depressions on the snow surface and the relation between the depressions and flow of meltwater. They report that snow grains were coarser (larger) in the depressions compared to surrounding snow and that the total outflow from rain gutters placed under the surface depressions was 5.4 times the outflow from areas outside of the depressions. Our results are not conclusive evidence that these valleys or depressions occur on the snow surface late in the melt season at an average spacing of 5-7 m. However, these results are intriguing and provide the impetus for further hypothesis testing.

The correlation lengths of the liquid water measurements of the snow surface suggest that the spatial distribution in the bimodal distribution of reflectance values was the result of greater liquid water content in the hollows or dark patches of the snow surface. It was quite surprising that we found any spatial structure in the spatial distribution of liquid water measurements at the snow surface. It was even more surprising that the two independent measurements resulted in the same correlation lengths of about 5-7 m. Moreover, it is quite encouraging that there appears to be some spatial structure to the wetness values at the snow surface.

The liquid water contents measured by the snow fork appear reasonable. Boyne and Fisk [1987] report that measurements of the liquid water content of the snow surface have an error of $\pm$ 2.3 cm^3 of H_2O per 100 cm^3 of snow, much less than the 0.5% difference we observed between mean values measured by the Denoth meter and the snow fork (n =

48). The mean value of 4.2% liquid water content measured by the snow fork during the comparison with the Denoth meter is also within the range measured by Kattelmann [1990] during the early stages of snow melt in the Sierra Nevada. Additionally, Pfeffer and Humphrey [1998] measured a liquid water content of 2-3% using the same snow fork (exact same instrument) along a segment of the equilibrium line in West Greenland. Measurements of the liquid water content of the snowpack made later in the melt season generally have values greater than 5% [Kattelmann, 1990]. The irreducible water content (analogous to the field capacity of soils) of a ripe and freely draining snowpack is generally considered to be 4 to 5% by most process-based snow melt models such as SNTHERM [Jordan, 1991]. The mean values of about 9% that we measured in late July on the snow surface therefore appear reasonable.

The amount of lysimeter outflow varied widely among lysimeters. Compared to the 1,016 mm of SWE measured at the index snowpit at maximum snow accumulation, five of the 16 lysimeters had annual outflows within 10%, six of the 16 lysimeters had annual outflows less than 10%, and five of the 16 lysimeters had annual outflows greater than 10% of the index snowpit. Two of the 16 lysimeters had quite high outflows, about 8 times and 16 times the SWE measured at the index snowpit. Most likely these high amounts of lysimeter outflow were the result of lateral flow within the snowpack from the gently-sloping snowpack to the west. At an alpine site in the eastern Sierra Nevada, Harrington and Bales [1998] report that annual discharges from eight 1-m^2 lysimeters ranged from 20% to 205% of the mean flow, an order of magnitude difference. However, that site was located on the top of a small tor and meltwater contribution from surrounding slopes did not occur. The extra contributing area that must account for the high lysimeter outflows at our site appears similar to the excess discharge that Kattelmann [1989] reports for lysimeter D that appeared to receive lateral flow from the surrounding snowpack.

Conflicting reports have appeared on whether meltwater flowpaths are re-used in a seasonal snowpack. Schneebeli [1995] reports that a dye study in the Alps of Europe showed that meltwater drained from the snow surface into a cold snowpack in preferential channels, but that these meltwater flowpaths froze and were not re-used. However, Wankiewicz [1979] strongly argues that meltwater does flow continuously through preferential areas in a ripe and draining snowpack. The multi-lysimeter work of Kattelmann [1989], Harrington and Bales [1998], and our study support the argument of Wankiewicz [1979] that more meltwater moves through some volumes of the snowpack relative to

other volumes of the snowpack.

The correlation lengths of 5-7 m that we report for the three independent measures of meltwater flow through snow are a statistical representation. We interpret these results to indicate that there is a higher density of meltwater flux on the scale of 5-7 m followed by areas with a lower density of meltwater flux every 5-7 m, as shown in Figure 1. These results do not mean that vertical flowpaths, pipes, or macropores occur on average every 5-7 m. In fact, our results suggest that areas of the snowpack with higher densities of meltwater flux most likely are composed of higher concentrations of macropore pipes or "bunches" or "bundles" of vertical flowpaths.

There will obviously be variance within a site. Most likely there will be a different statistical relationship for areas with different topography and/or climate. These results are not universal. However, they strongly suggest that meltwater flow through snow may have a spatial structure that is greater in "extent" then previously thought. The consistency of these statistical relationships is encouraging. It does appear that there is some spatial organization to the flow of meltwater through a ripe snowpack at the scale of 5-7 m in the central Rocky Mountains of the United States. Furthermore, Schneebeli [1998] reports that recent dye tracer experiments in the Swiss Alps of Europe showed preferential flowpaths through a melting snowpack on the scale of 5 m.

Dye tracer experiments have shown that meltwater produced at the top of the snowpack can move laterally through the snowpack at distances many times the snowpack depth before emerging as outflow at the base of the snowpack. The correlation lengths that we report for the three independent measurements of meltwater flow through snow are simple statistical structures and cannot imply causality. Nonetheless, a comparison of our results to unsaturated flow through soils may provide helpful insights and generate additional hypotheses regarding the physical processes that control meltwater flow through snow. Ruan and Illangesakare [1999, in press] have shown that microtopography plays a controlling role in the initiation of macropore flow in soils. Macropores located in depressions are initialized and remain active because of the larger amount of available water provided by topographic controls at the soil surface. In contrast, macropores on raised areas are not initialized or stop draining soon after initialization because there is less water available for infiltration. The snow surface may act in a somewhat analogous manner. There may be a high density of macropores or preferential flowpaths at the snow

surface, as suggested by the work of McGurk and Marsh [1995]. For a snowpack in the Sierra Nevada, they report flow fingers spaced about 20 to 40 mm apart, mean diameters of 15 to 20 mm, and a total wetted area of about 5%. Water infiltrating through these macropores from the surface into the interior of the snowpack may then become ponded on ice layers or fine-to-large grain transitions. Liquid water then moves laterally through the snowpack until breakthrough is achieved and vertical movement can continue. The snow overlying these vertical flowpaths then settles, creating a depression at the snow surface. There may then be a positive feedback system such that macropores in the resulting surface depressions carry more liquid water and macropores in the raised areas carry less liquid water, causing the depressions to become deeper and carry water from a larger contributing area. As the snowpack ripens, meltwater flowpaths then become correlated on the scale of meters.

CONCLUSIONS

Three independent techniques were used to test the hypotheses presented in the introduction: (1) low pass spatial filtering to identify multimodal brightness distributions in near infrared images of melting snowpacks; (2) variograms of the spatial distribution of meltwater from the bottom of melting snowpacks; and (3) capacitance measurements of the liquid water content of the upper surface of melting snowpacks. The three techniques support the hypotheses presented in the introduction.

[1] The characteristic distance separating bimodal reflectance peaks from aerial photographs of a draining snowpack in Colorado would be the same as that reported by Sommerfeld et al. [1994] for a Wyoming snowpack. The characteristic distances from the aerial photographs reported was approximately 6m.

[2] The frequency of bimodal distribution of brightness values from aerial photographs of snow covered area would increase from early in the melt season to later in the melt season. The probability of finding multimodal brightness distributions increased from 0.22 to 0.60 and 0.68, corresponding to the extent of snow melt.

[3] Direct measurements of the liquid water content of the snow surface will have the same characteristic distance as bimodal distributions of brightness values. Although there was a finer spatial structure evident in the liquid water measurements, regions of higher and lower liquid water content segregated into separate areas of about 5 m

in diameter. Variograms showed a sill at about 5 m and appeared to indicate an anti-correlation at about 10 m although the data at this distance is limited.

[4] The characteristic length of meltwater discharge measured in snow lysimeters at the base of the snowpack will have the same characteristic length as the bimodal brightness distribution of aerial photographs. Variograms indicate that correlation length of the meltwater collectors is 5 to 7 m and there is an indication that the melt is anti-correlated at about twice that distance.

These various spatial statistics are similar to those found in a preliminary study in the Snowy Range of Wyoming and indicate that a correlation length of 5-7 m for meltwater flow through a ripe snowpack may be of regional extent. An important result of this study is that infrared aerial photos can be used to investigate these spatial statistics over wide regions without labor intensive surface measurements. While these results are not conclusive, they do generate additional hypotheses on the spatial organization of meltwater flow through snow that warrant testing. In particular, these results support the contention of Bloschl [1999, in press] that the correlation lengths of meltwater flow through snow are greater than previous measurements made at the plot scale.

ACKNOWLEDGEMENTS

Tim Bardsley provided invaluable field help. Funding was provided by grants from the Army Research Office (DAAH04-96-1-0033 and DAAH04-96-0289), NSF Hydrology (EAR-9526875), the Niwot Ridge LTER program (NSF DEB 9211776), and NASA-EOS.

REFERENCES

Ahlmann, H. W., The stratification of the snow and firn on Isachsen's Plateau, *Geogra. Ann., 17*, 29-42, 1935.

Ahlmann, H. W. and A. Tveten, The recrystallization of snow into firn and the glaciation of the latter, *Geogra. Ann., 5*, 52-58, 1923.

Ambach, W., M. Blumthaler, and P. Kirchlechner, Application of the gravity flow theory to the percolation of melt water through firn, *J. Glaciol., 27*, 67-75, 1981.

Bloschl, G., Scaling issues in snow hydrology, *Hydrologic Processes*, 1999, in press.

Bloschl, G. and M. Sivapalan, Scale issues in hydrological modelling: A review, *Hydrologic Processes, 9*, 251-290, 1995.

Boyne, H. S. and D. Fisk, A comparison of snow liquid water measurement techniques, *Water Resour. Res., 23*, 1833-1836, 1987.

Caine, N., Streamflow patterns in the alpine environment of North Boulder Creek, Colorado Front Range, *Zeitschrift fur Geomorphologie, 104*, 27-42, 1996.

Cline, D., Effect of seasonality of snow accumulation and melt on snow surface energy exchanges at a continental alpine site, *J. of Applied Meteorology, 36*, 32-51, 1997.

Colbeck, S. C., One-dimensional water flow through snow, *Research Rep. 296*, Cold Regions Research and Engineering Laboratory, Hanover, NH, 1971.

Colbeck, S. C., A theory of water percolation in snow, *J. Glaciol., 11*, 369-385, 1972.

Colbeck, S. C., Theory of metamorphism of wet snow, *Research Rep. 313*, U.S. Army Cold Regions Res. Engrg. Lab., Hanover, NH, 1973.

Colbeck, S. C., A theory for water flow through a layered snowpack, *Water Resour. Res., 2*, 261-266, 1975.

Colbeck, S. C., An analysis of water flow in dry snow, *Water Resour. Res., 12*, 523-527, 1976.

Colbeck, S. C., Thermodynamic deformation of wet snow, *CRREL Rep. 76-44*, U.S. Army Cold Regions Res. Engrg. Lab., Hanover, NH, 1976.

Colbeck, S. C. and E. A. Anderson, Permeability of a melting snow cover, *Water Resour. Res., 18*, 904-908, 1982.

Davis, J. C., *Statistics and Data Analysis in Geology, 2nd ed.*, John Wiley & Sons, New York, 1986.

Denoth, A., A. Foglar, P. Weiland, C. Matzler, H. Aebischer, M. Tiuri, and A. Sihvola, A comparative study of instruments for measuring the liquid water content of snow, *J. Appl. Phys.*, *56*, 2154-2160, 1984.

Denoth, A., W. Seidenbusch, M. Blumthaler, P. Kirchlechner, W. Ambach, and S. C. Colbeck, Study of water drainage from columns of snow, *CRREL Rep. 79-1*, U.S. Army Cold Regions Res. Engrg. Lab., Hanover, NH, 1979.

Dozier, J., Estimation of properties of alpine snow from LANDSAT Thematic Mapper, *Adv. Space Res.*, *9*, 207-215, 1989.

Gerdel, R. W., *Physical changes in snow cover leading to runoff, especially to floods*, pp. 42-53, IAHS-AIHS Publication 31, Wallingford, U.K., 1948.

Gerdel, R. W., The transmission of water through snow, *Transactions, American Geophysical Union*, *35*, 475-485, 1954.

Harrington, R. K. and R. C. Bales, Interannual, seasonal, and spatial patterns of meltwater and solute fluxes in a seasonal snowpack, *Water Resour. Res.*, *34*, 823-831, 1998.

Higuchi, K. and Y. Tanaka, Flow pattern of meltwater in mountain snow cover, in *Hydrological Aspects of Alpine and High-Mountain Areas*, edited by J. W. Glen, IAHS Publ. No. 138, pp. 63-69, Intl. Assoc. Hydrol. Sci., Wallingford, UK, 1982.

Illangasekare, T. H., R. J. Walter Jr., M. F. Meier, and W. T. Pfeffer, Modeling of meltwater infiltration in subfreezing snow, *Water Resour. Res.*, *26*, 1001-1012, 1990.

Jordan, P., The snowmelt hydrology of a small alpine watershed, *M.S. Thesis*, University of British Columbia, Vancouver, 1978.

Jordan, P., Meltwater movement in a deep snowpack, 1, Field observations, *Water Resour. Res.*, *19*, 971-978, 1983a.

Jordan, P., Meltwater movement in a deep snowpack, 2, Simulation model, *Water Resour. Res.*, *19*, 979-985, 1983b.

Jordan, R., A one-dimensional temperature model for a snowcover: technical documentation for SNTHERM.89, *Special Rep. 657*, U.S. Army Cold Regions Res. Engrg. Lab., Hanover, NH, 1991.

Kattelmann, R., Variability of liquid water content in an alpine snowpack, in *A Merging of Theory and Practice : Proceedings / International Snow Science Workshop*, pp. 261-265, ISSW Workshop Committee, Bigfork, Montana, 1990.

Kattelmann, R. C., Macropores in snowpacks of Sierra Nevada, *Ann. Glaciol.*, *6*, 1985.

Kattelmann, R. C., Measurements of snow layer water retention, in *Cold Regions Hydrology Symposium*, Amer. Water Resour. Assoc., St. Paul, MN, 1986.

Kattelmann, R. C., Spatial variability of snowpack outflow at a Sierra Nevada site, *Ann. Glaciol.*, *13*, 1989.

Kattelmann, R. C., Water movement and ripening processes in snowpacks of the Sierra Nevada, *Ph.D Thesis*, Geography Department, Univ. Calif., Santa Barbara, CA, 1995.

Marsh, P., Ripening processes and meltwater movement in arctic snowpacks, *Ph.D. Thesis*, McMaster University, Hamilton, Ontario, 1982.

Marsh, P., Grain growth in a wet arctic snow cover, *Cold Regions Sci. Technol.*, *14*, 23-31, 1987.

Marsh, P., Flow fingers and ice columns in a cold snowcover, *Proc. Western Snow Conf.*, *56*, 105-112, 1988.

Marsh, P. and M.-k. Woo, Meltwater movement in natural heterogeneous snow covers, *Water Resour. Res.*, *21*, 1710-1716, 1985.

McGurk, B. J. and P. Marsh, Flow-finger continuity in serial thick-sections in a melting Sierran snowpack, in *Biogeochemistry of Seasonally Snow Covered Catchments*, edited by K. Tonnessen, M. W. Williams, and M. Tranter, IAHS-AIHS Publ. 228, pp. 81-88, Intl. Assoc. Hydrol. Sci., Wallingford, UK, 1995.

Nolin, A. and J. Dozier, Estimating snow grain size using AVIRIS data, *Remote Sensing of the Environment*, *44*, 231-238, 1993.

Oda, T. and K. Kudo, Properties of snow and its density, *Seppyo*, *3*, 109-121, 1941.

Pfeffer, W. T. and N. F. Humphrey, Formation of ice layers by infiltration and refreezing of meltwater, *Ann. Glaciol.*, *26*, 83-91, 1998.

Pfeffer, W. T., T. H. Illangasekare, and M. F. Meier, Analysis and modeling of melt-water refreezing in dry snow, *J. Glaciol.*, *36*, 238-246, 1990.

Pfeffer, W. T., T. H. Illangasekare, and M. F. Meier, Retention of Greenland runoff by refreezing: implications for projected future sea level change, *J. Geophys. Res.*, *96*, 22,117-22,124, 1991.

Rikkers, M., M. W. Williams, and R. Sommerfeld, Spatial statistics of meltwater flux at a continental alpine site, Rocky Mountains, *Proc. Western Snow Conf.*, 1996, in press.

Ruan, H. and T. H. Illangasekare, A model to couple overland flow and infiltration into macroporous vadose zone, *J. Hydrol.*, 1999, in press.

Schneebeli, M., Development and stability of preferential flow paths in a layered snowpack, in *Biogeochemistry of Seasonally Snow Covered Basins*, edited by K. A. Tonnessen, M. W. Williams, and M. Tranter, IAHS-AIHS Publ. 228, pp. 89-96, Intl. Assoc. Hydrol. Sci., Wallingford, UK, 1995.

Schneebeli, M., *Unsaturated water flow in snow: experiment and simulation*, US Army Cold Regions Research and Engineering Laboratory Special Report 98-10, p. 2, 1998.

Seligman, G., *Snow Structure and Ski Fields*, 555 pp., J. Adams, Brussels, 1936.

Sharp, R., Features of the firn on upper Seward Glacier, St. Elias mountains, Canada, *J. Geol.*, *59*, 599-621, 1951.

Shivola, A. and M. Tiuri, Snow fork for field determination of the density and wetness profiles of a snow pack., *IEEE Trans. Geosci. Remote Sens.*, *GE-24*, 717-721, 1986.

Sommerfeld, R. A., R. C. Bales, and A. Mast, Spatial statistics of snowmelt: data from lysimeters and aerial photos, *Geophysical Research Letters*, *21*, 2821-2824, 1994.

US Army Corps of Engineers,, Snow Hydrology; Summary of Report of Snow Investigations, *PB-151660*, North Pacific Division, Portland, Or., 1956.

Wakahama, G., The metamorphism of wet snow, *International Association of Hydrological Sci.s Publication*, *79*, 370-378, 1968*a*.

Wakahama, G., Infiltration of meltwater into snow cover III: Flowing down speed of melt water in a snow cover, *Low Temperature Sci.*, *26A*, 77-86, 1968*b*.

Wankiewicz, A., Water percolation within a deep snowpack--Field investigations at a site on Mt. Seymour, British Columbia, *unpublished Ph.D. dissertation*, University of British Columbia, Vancouver, 1976.

Wankiewicz, A., A review of water movement in snow, in *Proc. Modeling Snow Cover Runoff*, edited by S. C. Colbeck and M. Ray, U.S. Army Cold Regions Res. Engrg. Lab., Hanover, New Hampshire, 1979.

Williams, M. W., P. D. Brooks, A. Mosier, and K. A. Tonnessen, Mineral nitrogen transformations in and under seasonal snow in a high-elevation catchment, Rocky Mountains, USA, *Water Resour. Res.*, *32*, 3175-3185, 1996b.

Williams, M. W., D. Cline, M. Hartmann, and T. Bardsley, Data for snowmelt model development, calibration, and verification at an alpine site, Colorado Front Range, *Water Resour. Res.*, in review.

Williams, M. W., M. Losleben, N. Caine, and D. Greenland, Changes in climate and hydrochemical responses in a high-elevation catchment, Rocky Mountains, *Limnol. Oceanogr.*, *41*, 939-946, 1996a.

Williams, M. W. and J. M. Melack, Solute chemistry of snowmelt and runoff in an alpine basin, Sierra Nevada, *Water Resour. Res.*, *27*, 1575-1588, 1991.

Zar, J. H., *Biostatistical Analysis, Second Edition*, Prentice-Hall, Englewood Cliffs, N.J., 1984.

Figure 1. Planimetric and cross-sectional views showing theoretical flowpaths of liquid water in a ripe and draining snowpack, based on the conceptual ideas of Wankiewicz [1979] and Sommerfeld et al. [1994]. Pits or valley-shaped depressions are caused on the snow surface because of preferential settling of the overlying surface as liquid water penetrates to lower snow layers. The higher amounts of liquid water in the pit areas cause snow grains to grow faster and larger in the pit areas compared to surrounding raised areas. The higher absorption of light in the near-IR region by larger snow grains causes a decrease in albedo in the depressed areas compared to the raised areas, resulting in the snow surface having a checkerboard appearance caused by alternating light and dark areas. Accumulating lateral flow within the snowpack may then occur between the surface depressions, with greater flow amounts underneath the depressions. The distance between surface pits is the wavelength (λ) of a repeating spatial pattern. One-half λ would be the distance that features are correlated using geostatistical tests such as semivariograms.

Figure 2. Oblique aerial photograph taken in April near maximum snow accumulation. Niwot Ridge is the broadening ridge in the center of the photo and running left to right.

Figure 3. An illustration of how the frequency of brightness values changes by changing the cutoff wavelength of the Fourier filter from two different windows [adapted from Sommerfeld et al., 1994]. The x-axis is brightness value, the y-axis is frequency, and the far-left values are the wavelength of the spatial filter. At a wavelength of 1.5 m there is a single peak in the frequency of brightness values. As the size of the spatial filter increases the frequency distribution of brightness values changes, with a strongly bimodal distribution at a wavelength of 12 m or correlation length of 6 m.

Figure 4. Aerial photograph of snow covered area on Niwot Ridge, 14 June 1995. North is to the top of the scene and the photo was taken about 11 AM. The upper left and lower right areas are unaltered sections of the original frame. Black areas are non snow-covered area and the gray area is the snow surface. There is little patterning to the snow-covered area. The upper middle portion of the frame shows the image after the Fourier analysis with a 12-m spatial filter, which highlights dark and light patches on the snow

surface. We've highlighted one "window" located just to the upper right of the center of the frame. The window is approximately 150 pixels by 150 pixels, for a total of about 22,500 brightness measurements representing an area on the ground of 7,310 m^2. The inset on the lower left of the frame is a frequency diagram of brightness values for this window; the x-axis of the inset is brightness value and the y-axis is the number of pixels with that brightness value. There is a tri-modal distribution of brightness values shown in the inset histogram.

Figure 5. Probability of finding a bimodal distribution in the frequency of brightness values from aerial photographs of snow-covered area as a function of the stage of snow melt.

Figure 6. A histogram of brightness values from aerial photographs of snow-covered area, illustrating the bimodal distribution of brightness values. Note that there is a smaller peak in brightness values between the two main peaks. This smaller peak suggests that perhaps the correlation lengths in brightness values that we report of 5-7 m are composed of smaller flowpaths that are "bunched" into longer wavelengths.

Figure 7. A 3-dimensional surface plot of liquid water content of the snow surface from a 100 m^2 grid with 50-cm sampling resolution. The x and y axes are length (m) along the grid and the z-axis is percent liquid water content of the snow surface by volume, as measured with a dielectric Snow Fork.

Figure 8. A semivariogram of lag distance in m versus semivariance (γ_h) for measurements of the liquid water of the snow surface from a 10 m X 10 m grid and a 7.5 m X 10 m grid, each with measurements every 0.5 m.

Figure 9. Total measured discharge (mm) in each of the sixteen lysimeters for 1997. Maximum snow water equivalence (SWE) measured at the index snow pit was 1,016 mm. Discharge in lysimeters ranged from 42% of snowpit SWE to 16 times snowpit SWE.

Figure 10. Variogram for measured discharge for the 1997 and 1995 snowmelt seasons, normalized by dividing by the population variance. Measured lag distances ranged from

0 to 10 m.

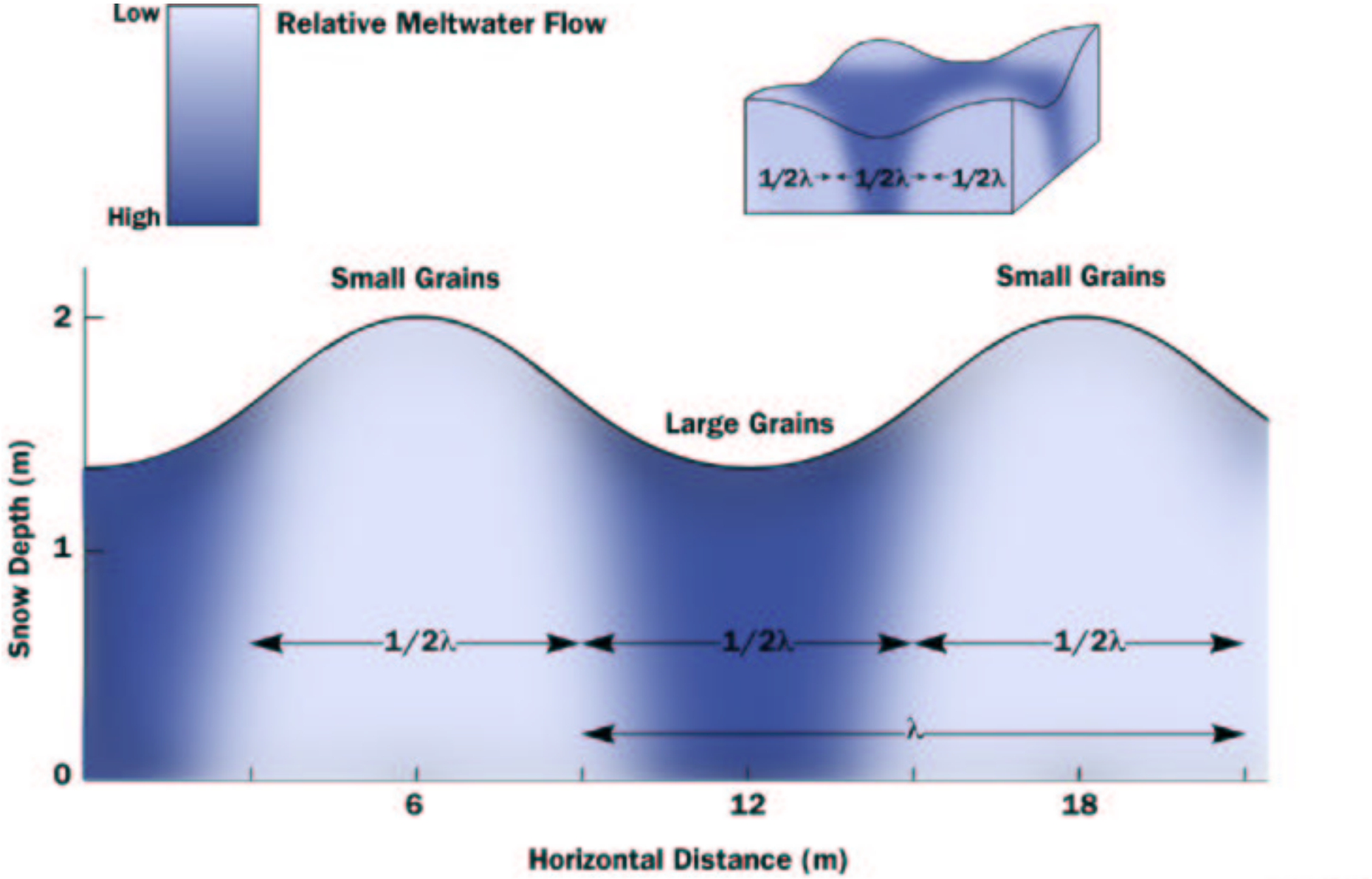

Williams, 9/98


Niwot Ridge
LTER Site
COLORA
Saddle Site

There is no electronic version of Figure 3.

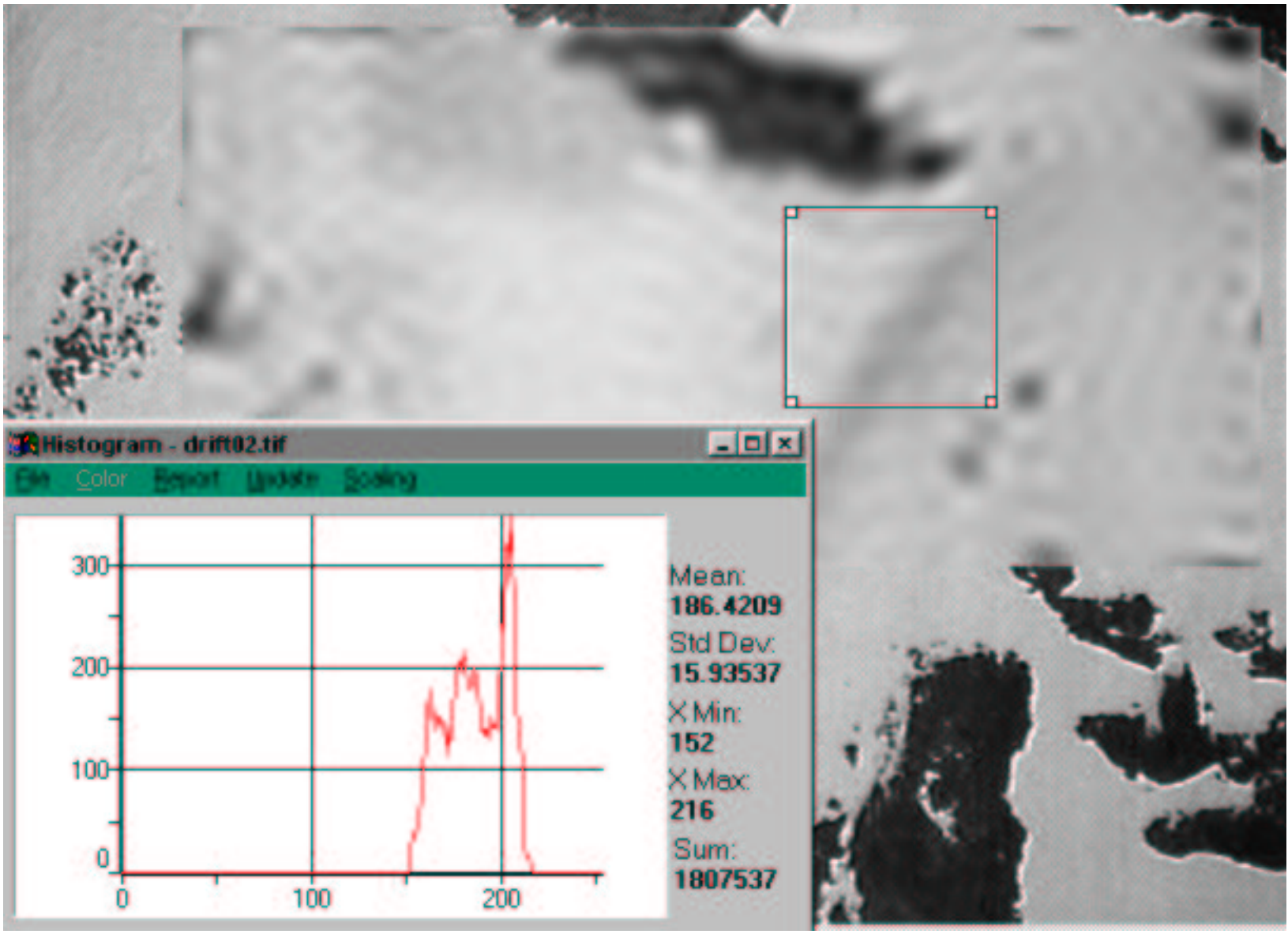
Histogram - drift02.tif
Color
300
200
100
0
0
100
200
Mean:
186.4209
Std Dev:
15.93537
X Min:
152
X Max:
216
Sum:
1807537

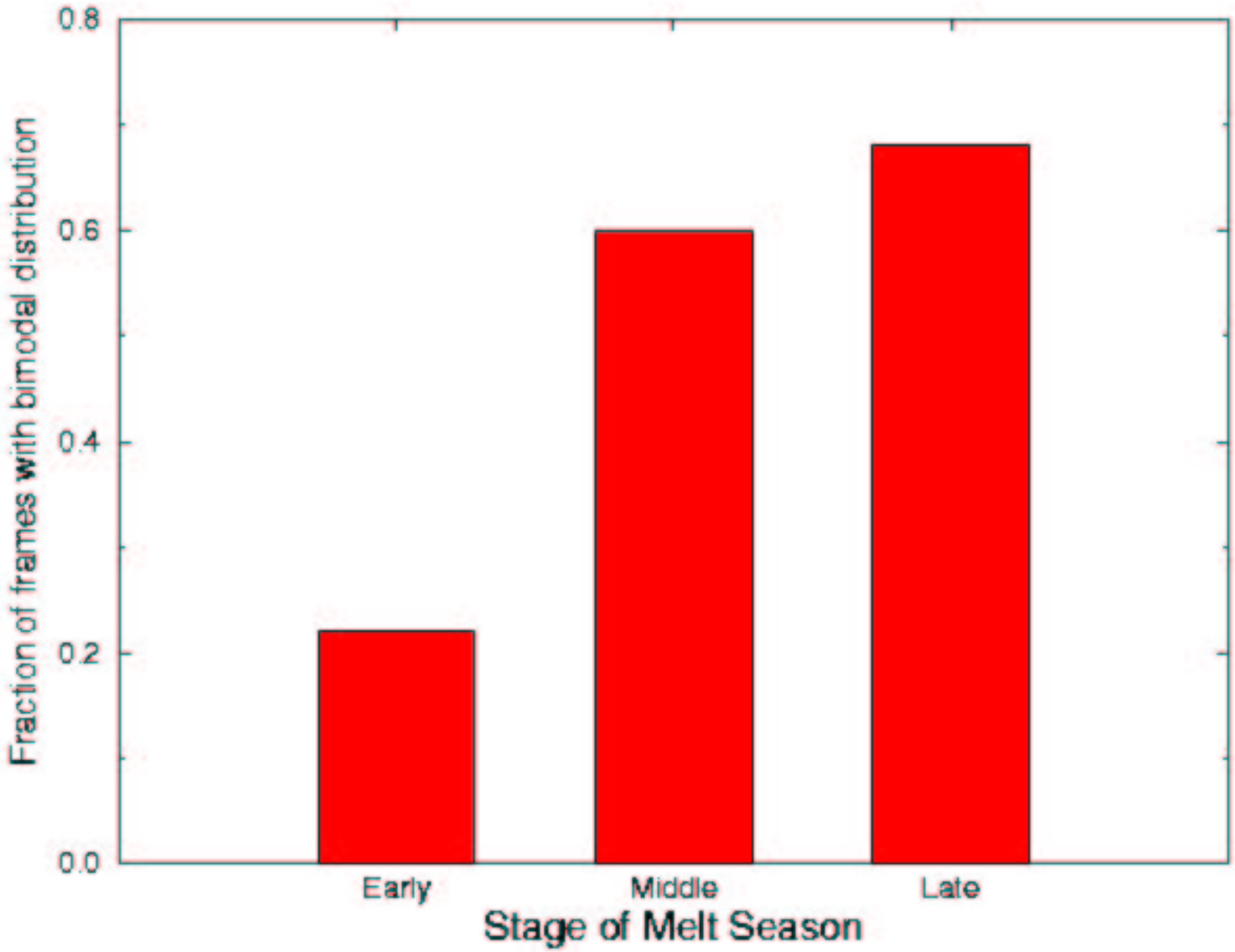
0.8
0.6
0.4
0.2
0.0
Fraction of frames with bimodal distribution
Early
Middle
Late
Stage of Melt Season

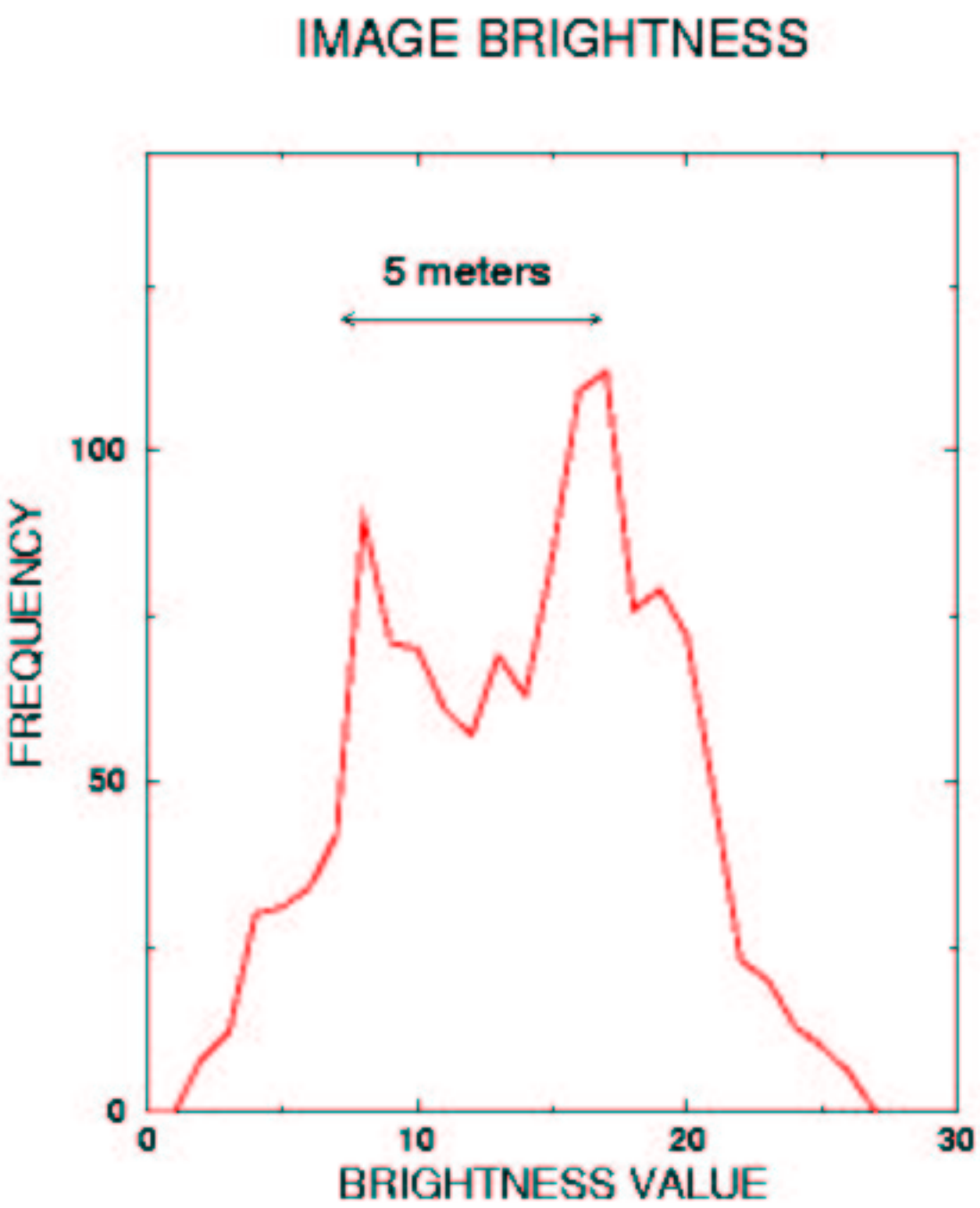
IMAGE BRIGHTNESS
5 meters
100
50
0
FREQUENCY
0
10
20
30
BRIGHTNESS VALUE

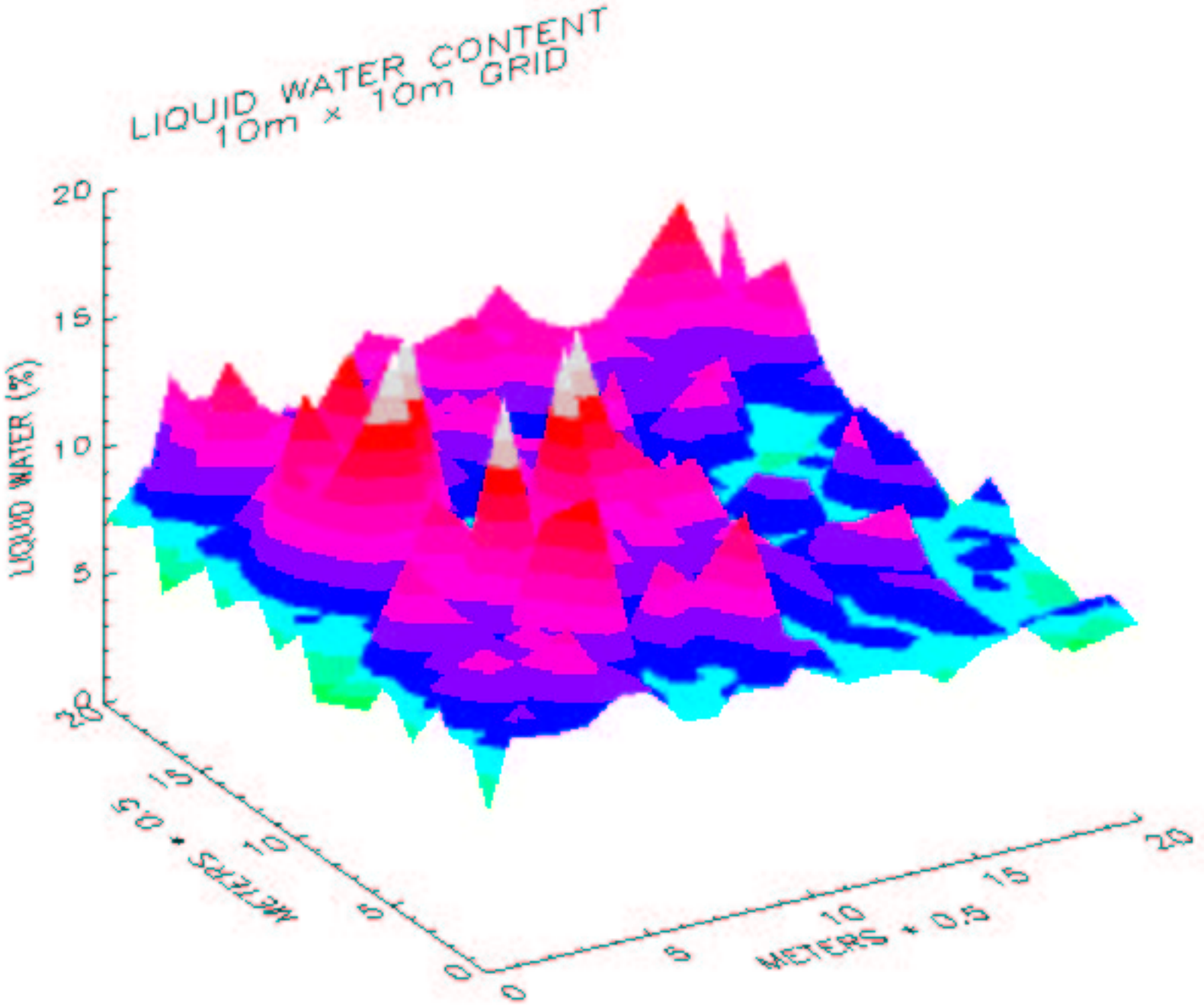
LIQUID WATER CONTENT
10m x 10m GRID
LIQUID WATER (%)
20
15
10
5
0
METERS * 0.5
0
5
10
15
20
METERS * 0.5
0
5
10
15
20

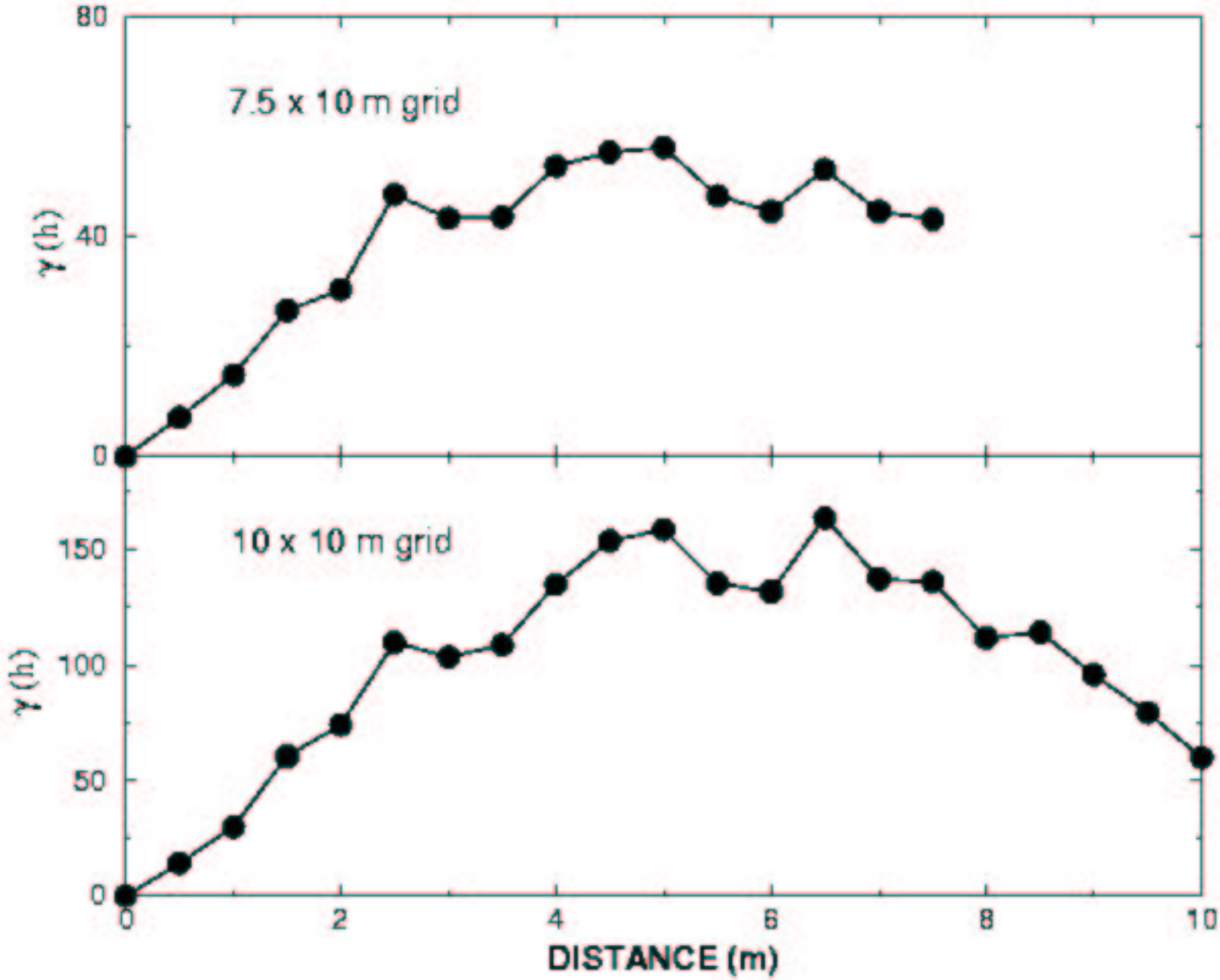
7.5 x 10 m grid
10 x 10 m grid
γ (h)
γ (h)
0
40
80
0
50
100
150
0
2
4
6
8
10
DISTANCE (m)

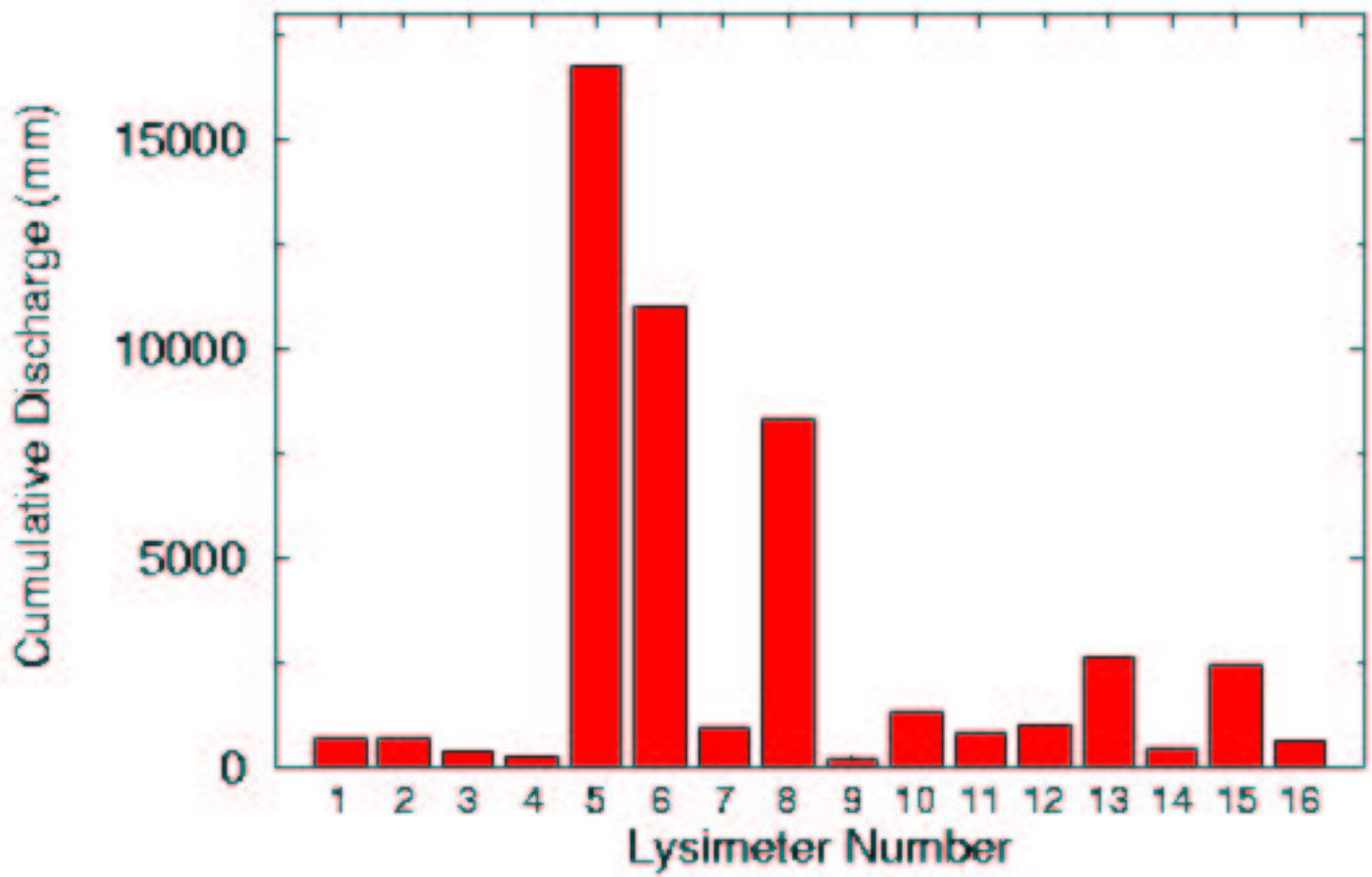
Cumulative Discharge (mm)
15000
10000
5000
0
1 2 3 4 5 6 7 8 9 10 11 12 13 14 15 16
Lysimeter Number

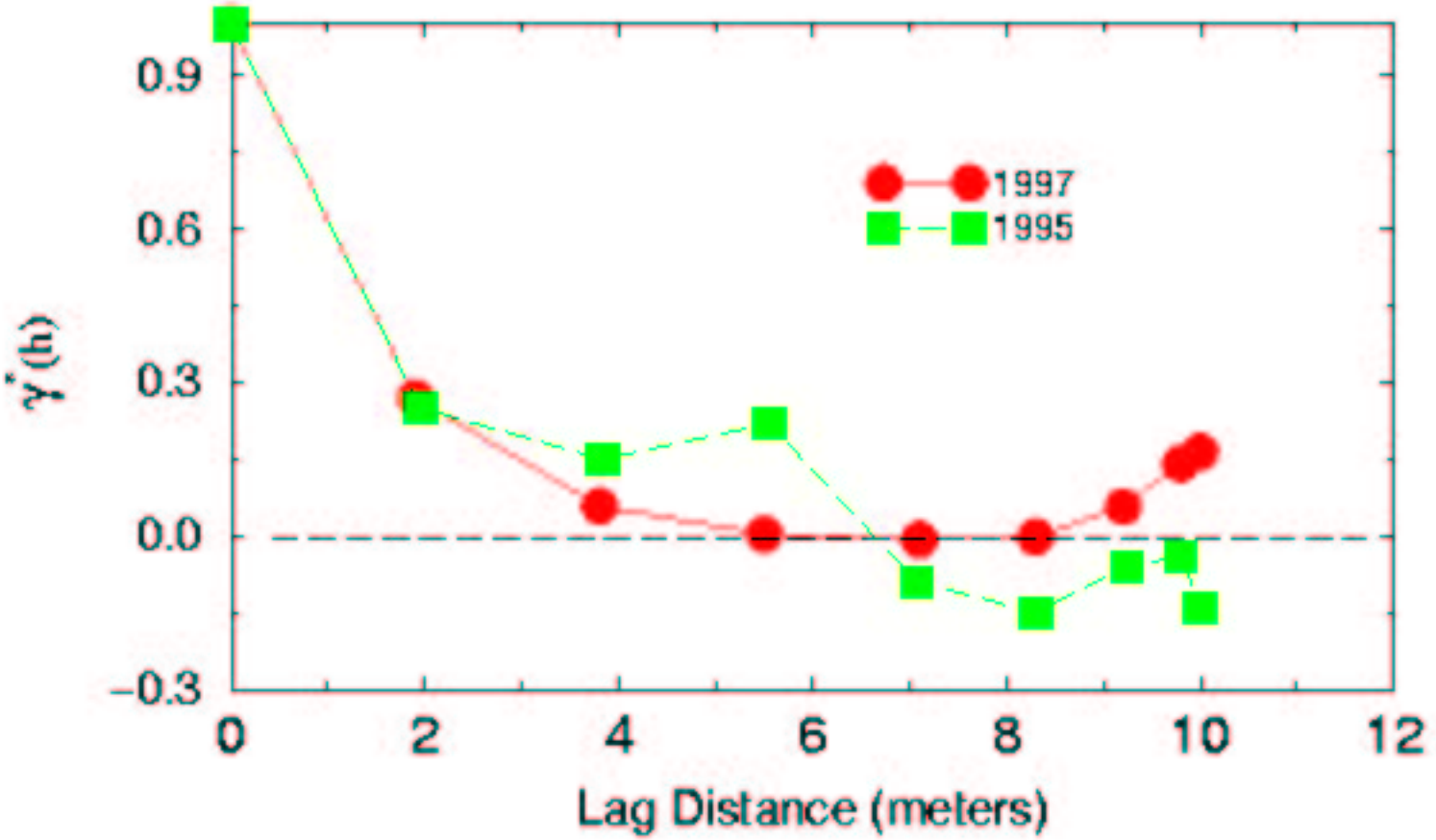
0.9
0.6
0.3
0.0
−0.3
0
2
4
6
8
10
12
γ*(h)
Lag Distance (meters)
1997
1995